J Mater Sci (2009) 44:4348–4353
DOI 10.1007/s10853-009-3649-7

Effect of annealing parameters on the magnetic properties of NiZn ferrite thin films

Ke Sun · Zhongwen Lan · Zhong Yu · Xiaoliang Nie · Lezhong Li · Xiaoning Zhao

Received: 28 October 2008 / Accepted: 28 May 2009 / Published online: 16 June 2009
© Springer Science+Business Media, LLC 2009

Abstract $Ni_{0.5}Zn_{0.5}Fe_{2.0}O_{4.0}$ thin films (NZFs) were deposited on Si (100) substrate by a sol–gel method, and the effects of annealing parameters on the structure and magnetic properties of the proposed films were investigated. Moderate heating rate was beneficial to the nucleation of NZFs. When the heating rate was 2 °C/min the saturation magnetization (M_s) achieved its maximum and the coercivity (H_c) reached its minimum. Both the crystallization and M_s of NZFs enhanced with increasing annealing time; however, H_c changed contrarily. High quenching temperature produced a large stress and consequently deteriorated magnetic properties. The optimal annealing parameters of NZFs were annealed at 700 °C, heating rate 2 °C/min, annealing time 1 h, and gradually cooled to room temperature. Finally, NZFs showed a high magnetization of 320 emu/cm^3 and low coercivity of 86 Oe.

Introduction

The application of the microwave devices [1] and thin film devices [2] of high frequency requires the ferrite thin films of high performance. NiZn ferrite possesses the advantages such as high resistivity, Curie temperature, low-temperature coefficient, and excellent properties of high frequency, which thus can be used for thin film devices of high frequency. The preparation methods of NiZn ferrite thin films (NZFs) include sol–gel [2–4], spin spray plating [5, 6], magnetron sputtering [7], pulsed laser deposition [8], and so on. The sol–gel method adopted in this article has the following features. First, the composition of films trends to be homogeneous and films have high quality. Second, the annealing temperature is low, and the microstructure and microcrystallite size of thin films can be controlled by the heat treatment. Lastly, the equipment is cheap and the high vacuum is not necessary.

It is a universally accepted fact that annealing parameters extremely influence the structure, surface morphology, and magnetic properties of thin films. Attempts have been made by researchers to investigate the effects of annealing temperature on the structure and magnetic properties of NZFs deposited by different technologies [2, 3, 7]. But all of them only investigated one of the annealing parameters, annealing temperature. We have previously reported the effects of annealing temperature on the structure and magnetic properties of NZFs [9]. In this study, one aims to investigate thorough the annealing parameters like heating rate, annealing time and quenching temperature on the structure, surface morphology, and magnetic properties of NZFs deposited by a sol–gel method.

Experimental procedures

Preparation of NiZn thin films

The samples of $Ni_{0.5}Zn_{0.5}Fe_{2.0}O_{4.0}$ thin films (NZFs) were deposited by a sol–gel method. Stoichiometric quantities of analytical grade $Zn(CH_3COO)_2 \cdot 2H_2O$, $Ni(CH_3COO)_2 \cdot 4H_2O$, and $Fe(NO_3)_3 \cdot 9H_2O$ were first dissolved in 2-methoxyethanol to form a mixed solution. After the solution was stirred for 1 h, the acetic acid was added to adjust the concentration of the solution to 0.2 mol/L.

K. Sun (✉) · Z. Lan · Z. Yu · X. Nie · L. Li · X. Zhao
State Key Laboratory of Electronic Thin Films and Integrated Devices, University of Electronic Science and Technology of China, Chengdu 610054, People's Republic of China
e-mail: shmily811028@126.com

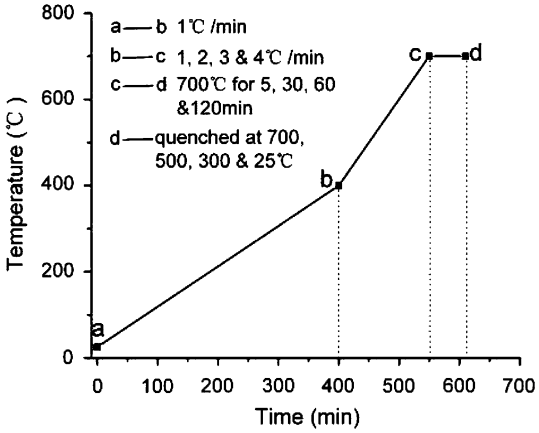

Fig. 1 The schematic diagram of temperature and time profiles for the annealing experiments

Simultaneously, polyethylene glycol was added. As a kind of surfactant, it can effectively prevent the colloidal particles of chelate compound from being jointed with each other. Then, the prepared solution was continuously stirred for 2 h and placed at room temperature for 36 h to form the stable sol–gel precursors used for the following processes. First, the wet films were deposited by a spin-coating method on the substrate of Si(100) with 4000 rpm for 30 s. Second, the wet films were dried at 100 °C for 10 min to remove the mixed solvents. Third, the operation of spin coating and drying was repeated to get the required thickness of the films. Lastly, the dried films were heated to 700 °C in air according to the schematic diagram of temperature and time profiles as indicated in Fig. 1. The thickness of the proposed films was about 140 nm.

Characterization and properties measurement

Thermal analysis by thermogravimetric analysis (TGA) and differential thermal analysis (DTA) was performed on the dried powders obtained from the $Ni_{0.5}Zn_{0.5}Fe_{2.0}O_{4.0}$ precursor solution. The phase identification of the thin films was performed by the Philips X'Pert PRO X-ray diffractometer (XRD), with Cu Kα radiation. The surface morphology of the films was analyzed by atomic force microscopy (AFM) and magnetic properties measurement by the TOEI VSM-5S-15 vibrating sample magnetometer (VSM) at room temperature.

Results and discussion

Thermo analysis (TGA/DTA) of dried gel for NiZn ferrite

Figure 2 shows the TGA–DTA plot of NiZn ferrite gel powder. It is observed from the TG curve that there are two

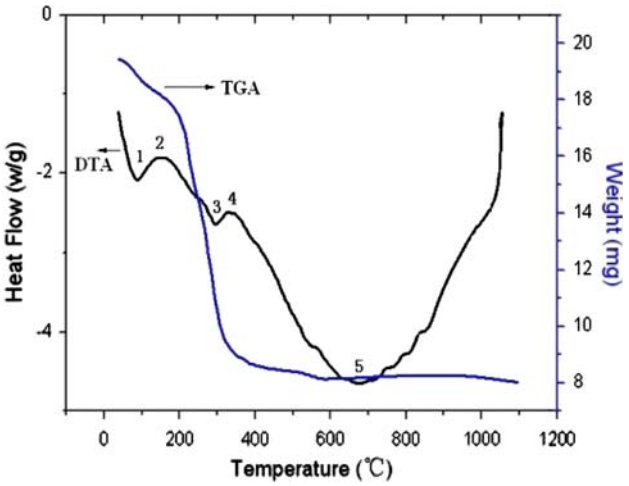

Fig. 2 TGA/DTA curves for $Ni_{0.5}Zn_{0.5}Fe_{2.0}O_{4.0}$ ferrite gel powder dried at 135 °C

stages. The gel exhibits a weight loss of 9.51% up to about 201 °C in the first (1st) stage, and shows a weight loss of 48.56% from 201 to 328 °C in the second (2nd) stage. The first stage is relatively mild, indicating the volatilization in organic solvent and water of crystallization. However, the second stage changes very cragged, implying the decomposition in organic salt and residual organic solvent. It is also observed from Fig. 2 that there are three endothermic peaks and two exothermic peaks. The endothermic peak 1 corresponds with the volatilization in organic solvent and water of crystallization, whereas the endothermic peak 3 corresponds with the decomposition in organic salts. The exothermic peaks 2 and 4 correspond with the decompositions of salts, and corresponding reactive equations are as follows:

$$4Fe(NO_3)_3 \rightarrow 2Fe_2O_3 + 12NO_2(g) + 3O_2(g) + \text{Heat} \quad (1)$$

$$Zn(CH_3COO)_2 + 2O_2 \rightarrow ZnO + 2CO_2(g) + 3H_2O(g) + \text{Heat} \quad (2)$$

$$Ni(CH_3COO)_2 + 4O_2 \rightarrow NiO + 4CO_2(g) + 3H_2O(g) + \text{Heat} \quad (3)$$

The endothermic peak 5 does not have obvious weight loss indicated from TG curve, which should be the crystallization of NiZn ferrite. It is found that the crystallization of NiZn ferrite occurs at about 560 °C, and corresponding reactive equation can be written as follows:

$$2Fe_2O_3 + NiO + ZnO \rightarrow 2Ni_{0.5}Zn_{0.5}Fe_{2.0}O_{4.0} \quad (4)$$

Effect of heating rate on the properties of NZFs

As shown in Fig. 2, the volatilization in organic solvents and the decomposition in salts have been accomplished before 400 °C. Therefore, in this study, one sets the

annealing temperature at 700 °C [9] for 1 h and then directly removes the samples. One investigates the effect of heating rate in the spectrum of 400–700 °C on the properties of NZFs. The heating rates are 1, 2, 3, and 4 °C/min.

Figure 3 demonstrates the hysteresis loops of NZFs annealed at 700 °C for 1 h as a function of heating rate (v). The hysteresis loops of NZFs for different v are typical ferrimagnetics. The saturation magnetization (M_s) and coercivity (H_c) of NZFs as a function of v are shown in Fig. 4. An initial increase followed by a subsequent decrease in M_s is observed with increase in v; however, H_c changes contrarily. The maximum M_s and minimum H_c of NZFs can be obtained when v is 2 °C/min. This study postulated that the crystallite growth of NZFs experienced the following stages: nucleation, islet, and network structure, and finally forming continuous films. The dependence between the nucleation probability and temperature is exponential [10]. The slower is the heating rate, the less are the nucleation numbers.

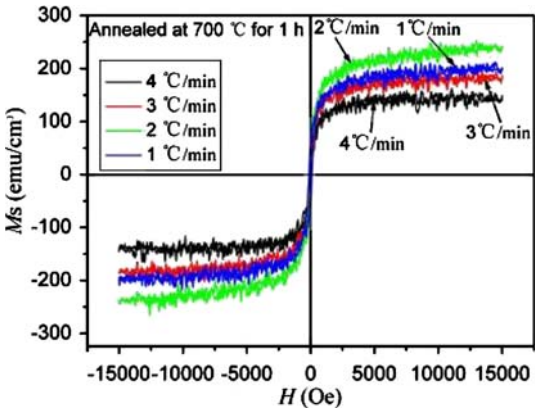

Fig. 3 Hysteresis loops of NZFs annealed at 700 °C for 1 h with different heating rates

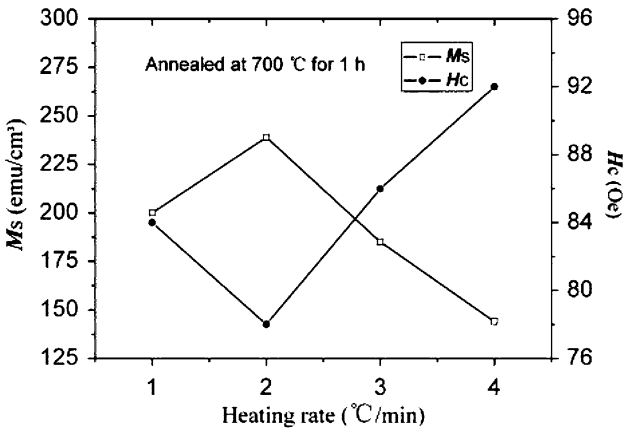

Fig. 4 M_s and H_c of NZFs annealed at 700 °C for 1 h with different heating rates

A new nucleation trends to stay at the edge of the formed nucleation in order to reduce the nucleation energy. M_s is defined as the vector sum of magnetic moment per unit cell, and is written as follows:

$$M_s = \frac{8M}{a^3}, \tag{5}$$

where M is the magnetic moment of molecule and a is the lattice parameter. Therefore, the slower heating rate results in a lower M_s. With the increase in heating rate, the nucleation energy of NZFs is sufficient, leading to a drastic increase in nucleation number. It is beneficial to forming the continuous films because nucleation of NZFs grows not too big in a short time, resulting in an enhancement in M_s and a decrease in H_c. Up to a higher heating rate (4 °C/min), there are two points leading to the deterioration of magnetic properties. On the one hand, the stress of NZFs under a higher heating rate cannot be released in time. On the other hand, the mismatch of heat expansion coefficient between NZFs and substrate at a high rate behaves more distinct than that at a low heating rate. Thus, in the subsequent research on the annealing time, one fixes the heating rate as 2 °C/min.

Effect of annealing time on the properties of NZFs

Figure 5 shows the XRD patterns of NZFs annealed at 700 °C for different annealing time (t). NZFs annealed at 700 °C for different t are crystallized. While t is 5 min, only the (311) diffraction peak of NZFs can be observed. It is weaker than that of NZFs for extending t, indicating the

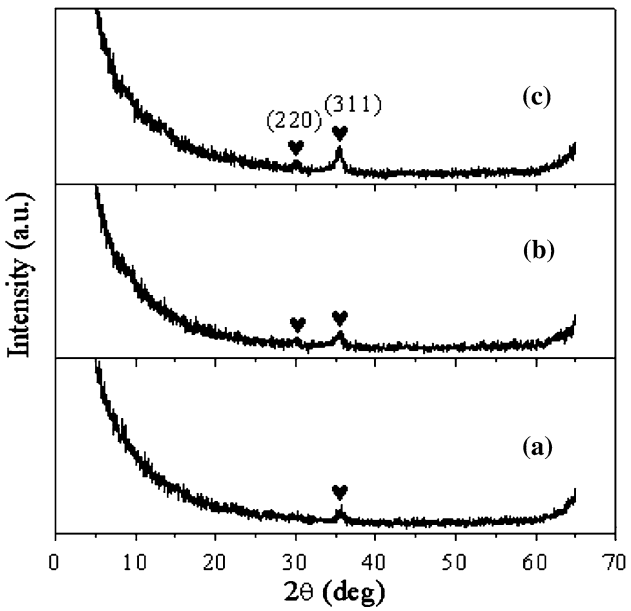

Fig. 5 XRD patterns of NZFs annealed at 700 °C for different annealing time (t). (a) 5 min, (b) 30 min, and (c) 120 min

appearance for a small amount of NZFs. The crystallization of NZFs enhances with increasing t. When t is 30 min, both the (220) and (311) diffraction peaks appear. Up to a higher t (120 min), the diffraction intensities of NZFs both in (220) and (311) peaks achieve their maxima, implying the best crystallization in our experimental range in t.

Figure 6 demonstrates the AFM images of NZFs annealed at 700 °C for various annealing time. The crystallite growth is strongly dependent on the annealing time (t). Only a few of crystallites can be observed when t is 5 min, which is consistent with the measurement of XRD as shown in Fig. 5a. The numbers of crystallites increase with increasing t, which is attributed to enough energy that atoms obtained, simultaneously leading to a further crystallite growth. When t is 60 min both the crystallite numbers and sizes increase.

Figure 7 shows the M_s and H_c of NZFs annealed at 700 °C for different annealing time (t). When t is ≤60 min, M_s increases rapidly with increasing t. However, H_c varies contrarily. Up to a higher t, M_s increases slowly but H_c is almost identical to that of 60 min. In combination with the previous analyses in crystal structure and surface morphology, it is not difficult to comprehend the variations in M_s and H_c. It can be explained through crystallite growth of NZFs: the increase in annealing time results in an enhancement in crystallization, an increase in crystallite size, and a decrease in volume of grain boundary, which are beneficial to proceeding of magnetization of NZFs and thus lead to an increase in M_s and a decrease in H_c. It is well acknowledged that long annealing time also brings on the increasing roughness, resulting in the properties deterioration of NZFs. In the subsequent research on the quenching temperature, one sets the annealing time at 60 min.

Effect of quenching temperature on the properties of NZFs

Figure 8 shows the XRD patterns of NZFs annealed at 700 °C for 1 h and then quenched at different temperatures

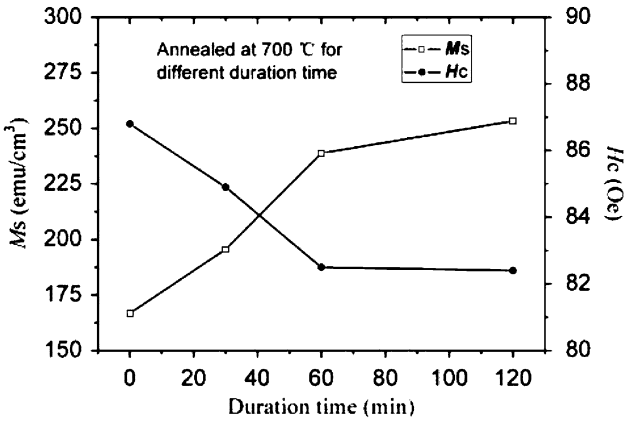

Fig. 7 M_s and H_c of NZFs annealed at 700 °C for different annealing time

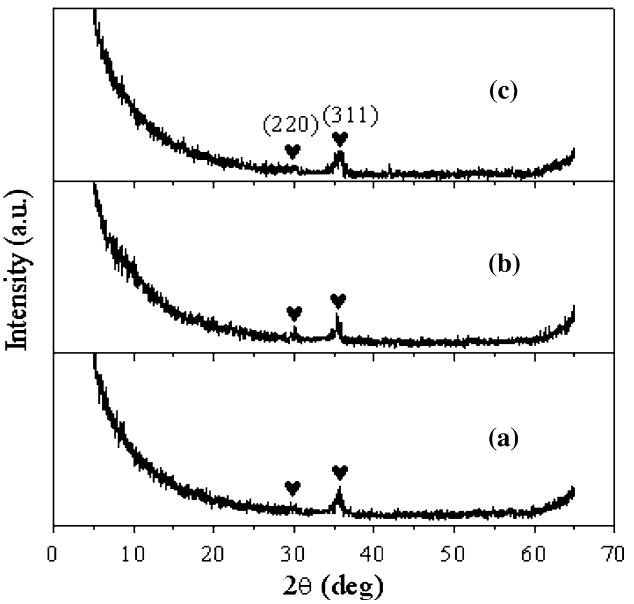

Fig. 8 XRD patterns of NZFs annealed at 700 °C for 1 h as a function of quenching temperature. (a) 25 °C, (b) 300 °C, and (c) 700 °C

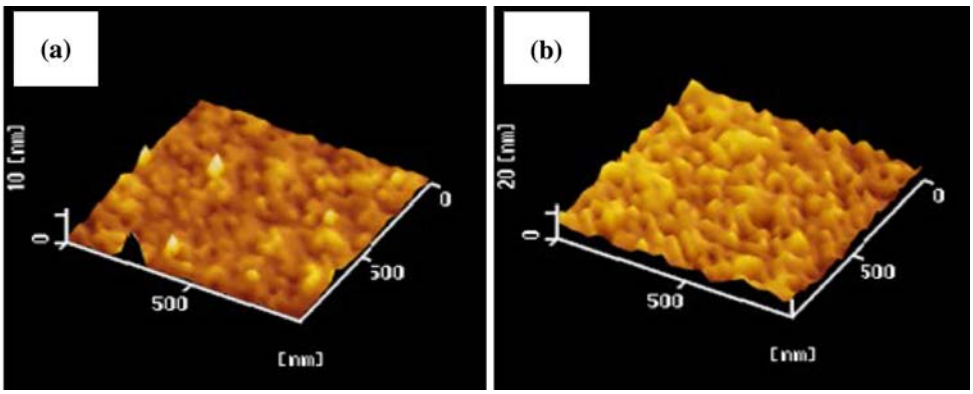

Fig. 6 AFM images of NZFs annealed at 700 °C for different annealing time (t). (a) 5 min, (b) 60 min

(T_q), b, c quenched at 300 and 700 °C, respectively, a is gradually cooled to room temperature in the furnace. NZFs annealed at 700 °C for different T_q are crystallized and T_q does not have obvious difference in the intensity of diffraction peaks, indicating there is no distinct effect in crystallization of NZFs. It is also found that NZFs quenched at different T_q have cubic spinel structure and without unidentified extra peaks. Thus, NZFs can be obtained at different T_q.

Figure 9 demonstrates the M_s and H_c of NZFs quenched at different temperatures. It can be clearly observed that M_s decreases with increasing T_q. However, H_c changes contrarily. During quenching process, atoms cannot come back to the ideal crystal due to the saltation of materials from high T_q to low T_q. In this case, the crystal lattices keep at the state of high energy, resulting in a decrease in difference of magnetic moment between A and B sublattices. In addition, there is a big stress inside the NZFs, and the congealed inner stress in NZFs grows bigger with increasing T_q. The higher is T_q and the faster is the cooling rate, which makes that the mismatch of heat expansion coefficient between NZFs and substrate becomes more obvious than that gradually cooled to room temperature, producing a big thermal stress. When the stress increases to a certain extent, NZFs could produce cracks and porosity, and at the same time the roughness increases. From the previous analyses about quenching temperature, it can be concluded that high quenching temperature would produce large stress and consequently deteriorate the properties of NZFs. With the decrease in quenching temperature, accompanying the stress release in NZFs, the properties of NZFs can be improved.

NZFs shows a high magnetization 320 emu/cm^3 and a low coercivity 86 Oe with optimal annealing parameters, which are annealed at 700 °C, heating rate 2 °C/min, annealing time 1 h, and gradually cooled to room temperature. Compared with references [7] and [11], one can prepare the high performance NZFs at a lower annealing temperature 700 °C. Desai et al. [7] deposited $Ni_{0.5}Zn_{0.5}Fe_{2.0}O_{4.0}$ films on Si(100) by RF magnetron sputtering. While NZFs were annealed at 800 °C, NZFs showed the optimal magnetic properties, $M_s = 250$ emu/cm^3, $H_c = 80$ Oe. Gao et al. [11] deposited $Ni_{0.5}Zn_{0.5}Fe_{2.0}O_{4.0}$ films on Si(100) by alternative sputtering technology. When NZFs annealed at 850 °C, NZFs had a high magnetization 360 emu/cm^3 and a low coercivity 106 Oe. The magnetization is a little higher than our experimental results, but the coercivity is also a little higher than our results. However, the most important here is that one can use the sol–gel method to prepare high performance NZFs at a low annealing temperature.

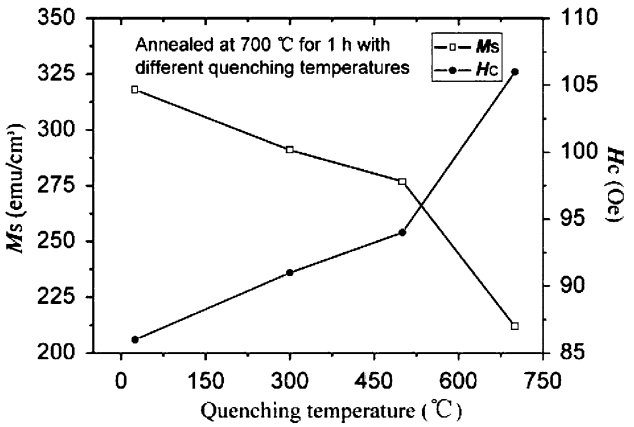

Fig. 9 M_s and H_c of NZFs annealed at 700 °C for 60 min with different quenching temperatures

Conclusions

NZFs were deposited on Si(100) substrate by a sol–gel method. The annealing parameters were investigated and the following results were obtained:

(1) Moderate heating rate is beneficial to the nucleation of NZFs. When the heating rate is 2 °C/min magnetization achieves its maximum and coercivity reaches its minimum.
(2) The crystallization of NZFs becomes intensified with increasing annealing time. The magnetization increases with increasing annealing time, but coercivity varies contrarily.
(3) High quenching temperature produces a large stress and consequently deteriorates magnetic properties of NZFs.
(4) The optimal annealing parameters of NZFs are annealed at 700 °C, heating rate 2 °C/min, annealing time 1 h, and gradually cooled to room temperature. Finally, NZFs show a high magnetization 320 emu/cm^3 and a low coercivity 86 Oe.

Acknowledgements The authors would like to thank Prof. Y. Jin for the XRD measurements and Mr. Y. F. Tian for the AFM measurements and their helpful discussion.

References

1. Williams CM, Chrisey DB, Lubitz P, Grabowski KS, Cotell CM (1994) J Appl Phys 75:1676
2. Liu F, Ren TL, Yang C, Liu LT, Wang AZ, Yu J (2006) Mater Lett 60:1403
3. Bae SY, Kim CS, Oh YJ (1999) J Appl Phys 85:5226
4. Sun K, Lan ZW, Yu Z, Nie XL, Li LZ, Liu CY (2008) J Magn Magn Mater 320:1180
5. Matsushita N, Nakamura T, Abe M (2003) J Appl Phys 93:7133
6. Fu CM, Hsu HS, Chao YC, Matsushita N, Abe M (2003) J Appl Phys 93:7127

7. Desai M, Prasad S, Venkataramani N, Samajdar I, Nigam AK, Keller N, Krishnan R, Baggio-Saitovitch EM, Pujada BR, Rossi A (2002) J Appl Phys 91:7592
8. Chinnasamy CN, Yoon SD, Yang A, Baraskar A, Vittoria C, Harris VG (2007) J Appl Phys 101:1
9. Sun K, Lan ZW, Nie XL, Yu Z, Zhao XN, Li LZ (2009) Yadian Yu Shengguang 31(5) (in Chinese)
10. Yu QY, Zhang JX (2002) ACTA Scientiarum Naturalium Universities Sunyatseni 41(4):34 (in Chinese)
11. Gao JH, Cui YT, Yang Z (2004) Mater Sci Eng B 110(2):111